Supporting Information for "Transient Warming is More Sensitive to Uncertainty in the Forcing than to Uncertainty in the Radiative Feedbacks"

N. J. Lutsko,[1]

Max Popp[2]

Contents of this file

1. Text S1 and S2

Corresponding author: N. J. Lutsko, Department of Earth, Atmospheric, and Planetary Sciences, Massachusetts Institute of Technology, Cambridge, Massachusetts, USA. (lutsko@mit.edu)

[1]Department of Earth, Atmospheric, and Planetary Sciences, Massachusetts Institute of Technology, Cambridge, Massachusetts, USA.

[2]Laboratoire de Météorologique Dynamique Dynamique, Sorbonne Université, Ecole Normale Supérieure, Ecole Polytechnique, Paris, France.

2. Tables S1 to S3

3. Figures S1 to S2

Introduction The supplementary material contains two text sections, three tables and two figures. The first text section provides details on how the EBM was fit to the CMIP5 data. The second text section describes where the historical forcing data was obtained from and how the EBM was fit to historical global-mean surface temperatures. The first table defines the terms in the analytic solution to the EBM; the second table lists the CMIP5 models used in this study and their corresponding values of F, λ, c, c_0, γ, TCR and ECS; and the third table shows r^2 values for correlations between the five parameters of the EBM across the CMIP5 models. The first figure compares time-series of global-mean surface temperature from CMIP5 model runs with CO_2 concentrations increasing by 1% per year and fits of the EBM to these simulations. The second figure repeats Figure 1 of the main text, but for the alternative form of the EBM which includes ϵ, a measure of the efficacy of ocean heat uptake.

Text S1. Fitting and integrating the energy balance model The EBM was fitted to each model using the same two-step procedure as *Geoffroy et al.* [2013a]. In the first step, F and λ are estimated using the *Gregory et al.* [2004] method by linearly regressing the net TOA radiative imbalance (R) in the quadrupled CO_2 experiments versus the global-mean surface temperature (T). The forcing F is then equal to the y-intercept of the regression and λ is equal to the slope of the regression.

For $t >> \tau_F$, the solution to the EBM can be written as

$$T_1 \approx ECS(1 - a_s e^{-t/\tau_s}), \tag{1}$$

and so

$$log(1 - \frac{T_1}{ECS}) \approx log(a_s) - \frac{1}{\tau_s} t. \tag{2}$$

Provided that $\tau_F << 30$ years, a_s and τ_s can be estimated from the linear regression of $log(1 - \frac{T_1}{ECS})$ versus t for the quadrupled CO_2 experiments. $a_f = 1 - a_s$, and τ_f can be expressed as

$$\tau_f = t / \left[log(a_f) - log(1 - T_1/ECS - a_s e^{-t/\tau_s}) \right], \tag{3}$$

which can be estimated by averaging over the first ten years of the step-forcing experiment. The heat capacities and γ can be computed from the other parameters.

Integrations of the EBM were performed using backwards Euler time-stepping, with a time-step of one year. The results are not sensitive to the choice of time-step or the choice of numerical integration scheme.

Text S2. Fitting the 20th Century

The 20th century surface temperature is taken from the HADCRUT4 dataset, available at https://crudata.uea.ac.uk/cru/data/temperature/, and the greenhouse gas concentrations were downloaded from http://www.pik-potsdam.de/∼mmalte/rcps/. The radiative forcing due to CO_2 was again calculated as $\Delta F_{CO2}(t) = F_{CO2} log(C(t)/C_0)$, while the forcings due to NO_2 and CH_4 were both estimated as $\Delta F_X(t) = F_X(\sqrt{X(t)} - \sqrt{X(0)})$ [*Etminan et al.*, 2016]. We take a mean value of F_{NH4} of 0.117 Wm^{-2} and of F_{CH4} of $0.043\mathrm{Wm}^{-2}$ [*Etminan et al.*, 2016], and assume that each of these has the same relative uncertainty as F_{CO2}.

To find the optimal value of λ the calculations were repeated for all values of λ between 0.01 and $3\mathrm{Wm}^{-2}\mathrm{K}^{-1}$, in increments of $0.01\mathrm{Wm}^{-2}\mathrm{K}^{-1}$, and then the optimal value was taken as the value of λ which produced the time-series of T_1 with the smallest root-mean-squared error compared to the observed temperature record.

References

Etminan, M., G. Myhre, E. J. Highwood, and K. P. Shine (2016), Radiative forcing of carbon dioxide, methane, and nitrous oxide: A significant revision of the methane radiative forcing, *Geophysical Research Letters*, *43*(24), 12,614–12,623.

Geoffroy, O., D. Saint-Martin, G. Bellon, A. Voldoire, D. J. L. Olivie, and S. Tyteca (2013a), Transient climate response in a two-layer energy-balance model. part i: Analytical solution and parameter calibration using cmip5 aogcm experiments, *Journal of Climate*, *26*(6), 1841–1859.

Gregory, J. M. , W. J. Ingram, M. A. Palmer, G. S. Jones, P. A. Stott, R. B. Thorpe, J. A. Lowe, T. C. Johns, and K. D. Williams. (2004), A new method for diagnosing radiative forcing and climate sensitivity., *Geophysical Research Letters*, *31*(9), L03205

Table S1. Definitions of terms in analytic solution to the EBM.

Fast terms:	Slow terms:
$a_f = \frac{\phi_s \tau_f}{c(\phi_s - \phi_f)}\lambda$	$a_s = \frac{\phi_f \tau_s}{c(\phi_s - \phi_f)}\lambda$
$\phi_f = \frac{c}{2\gamma}(b^* - \sqrt{\delta})$	$\phi_s = \frac{c}{2\gamma}(b^* + \sqrt{\delta})$
$\tau_f = \frac{cc_0}{2\lambda\gamma}(b - \sqrt{\delta})$	$\tau_s = \frac{cc_0}{2\lambda\gamma}(b + \sqrt{\delta})$
Other terms:	
$b = \frac{\lambda+\gamma}{c} + \frac{\gamma}{c_0}$	
$b^* = \frac{\lambda+\gamma}{c} - \frac{\gamma}{c_0}$	
$\delta = b^2 - 4\frac{\lambda\gamma}{cc_0}$	

Table S2. The models used in this study and their corresponding values of F (units = $\mathrm{Wm^{-2}}$), λ ($\mathrm{Wm^{-2}K^{-1}}$), c ($\mathrm{Wm^{-2}K^{-1}s^{-1}}$), c_0 ($\mathrm{Wm^{-2}K^{-1}s^{-1}}$) and γ ($\mathrm{Wm^{-2}K^{-1}}$), as well as each model's TCR (K) and ECS (K).

Model	F	λ	c	c_0	γ	TCR	ECS
BCC-CSM1-1	3.3	1.21	7.6	53.	0.67	1.7	2.8
BNU-ESM	3.7	0.93	7.4	90.	0.53	2.2	4.0
CanESM2	3.8	1.03	7.3	71	0.59	2.4	3.7
CNRM-CM5	3.6	1.11	8.4	99	0.5	2.1	3.5
CSIRO-Mk3-6-0	2.55	0.61	6	69	0.88	1.8	4.1
FGOALS-s2	3.8	0.88	7	127	0.76	2.4	4.3
GFDL-CM3	3.05	0.75	9.2	88	0.68	2.0	4.1
GFDL-ESM2G	3.3	1.4	6.0	95	0.9	1.1	2.4
GFDL-ESM2M	3.3	1.34	8.1	105	1.3	1.3	2.4
GISS-ESM-LR	3.7	1.7	4.7	126	1.16	1.5	2.2
HADGEM2-ES	2.9	0.65	6.5	82	0.55	2.5	4.5
INMCM4	3.1	1.51	8.6	317	0.65	1.3	2.1
IPSL-CM5A-LR	3.2	0.79	7.7	95	0.59	2.0	4.1
MIROC5	4.3	1.58	8.3	145	0.76	1.5	2.7
MPI-ESM-LR	4.2	1.14	7.3	71	0.72	2.0	3.7
MRI-CGCM3	3.3	1.26	8.5	64	0.66	1.6	2.6
NCAR-CCSM4	3.6	1.24	6.1	69	0.93	1.8	2.9
NorESM1-M	3.1	1.11	8	105	0.88	1.4	2.8

Table S3. r^2 for correlations across models between each of the five parameters of the EBM.

r^2	F	λ	c	c_0	γ
F	1				
λ	0.21	1			
c	0.00	0.00	1		
c_0	0.00	0.18	0.05	1	
γ	0.00	0.23	0.37	0.00	1

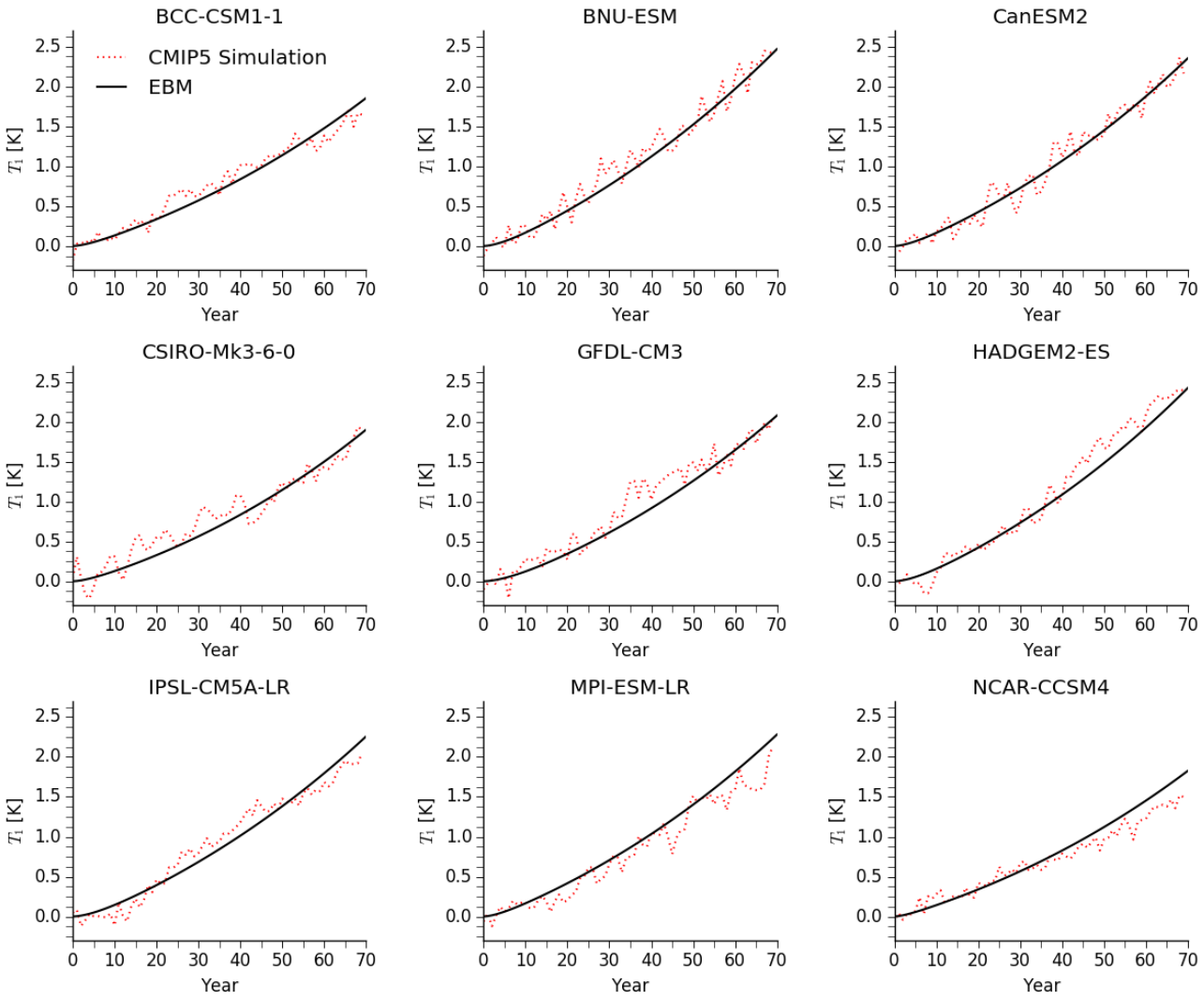

Figure S1. Time series of anomalous global-mean surface temperature in the 1% CO_2 simulations with nine of the models analyzed in this study (dotted red lines) and corresponding simulations with the EBM (solid black lines).

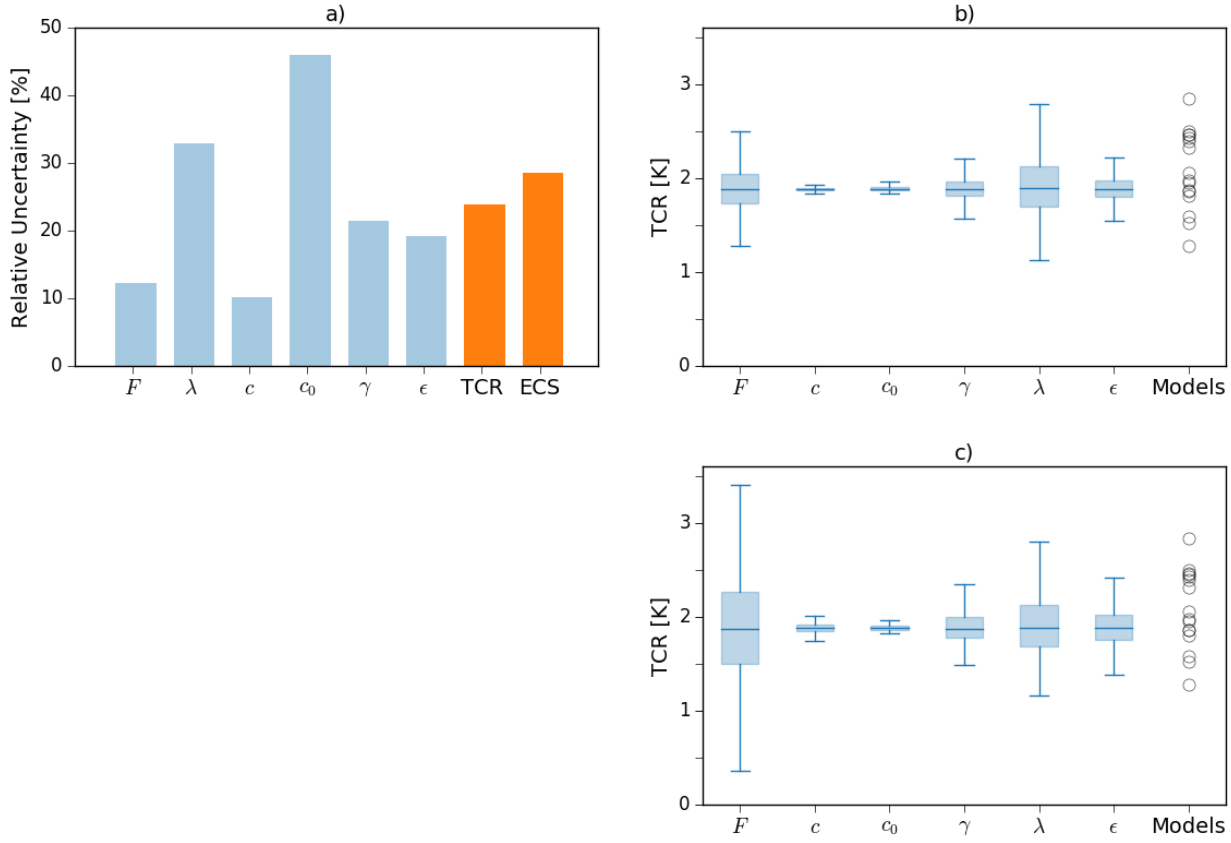

Figure S2. a) The relative uncertainties in each of the six parameters of the EBM that includes the effects of ocean heat uptake (blue bars), based on fitting the EBM to the 18 CMIP5 models, as well as the uncertainties in the ECS and the TCR (orange bars). b) Box-and-whisker plots showing the distributions of TCR from the Monte-Carlo analysis. The boxes show ±one standard deviation, the horizontal lines show the mean and the whiskers bracket the 5-95% confidence intervals. The round markers show the models' TCRs. c) Same as panel b) but the Monte Carlo analysis is performed assuming the same relative uncertainty for each parameter.